PHYSICAL REVIEW B, VOLUME 65, 180404(R)

Stroboscopic detection of nuclear forward-scattered synchrotron radiation

R. Callens,[1,*] R. Coussement,[1,2] C. L'abbé,[1,3] S. Nasu,[4] K. Vyvey,[1] T. Yamada,[5] Y. Yoda,[5] and J. Odeurs[1]
[1]*Instituut voor Kern- en Stralingsfysica, K.U. Leuven, Celestijnenlaan 200D, B-3001 Leuven, Belgium*
[2]*Université Libre de Bruxelles, Campus Plaine CP 231, boulevard du Triomphe, B-1050 Bruxelles, Belgium*
[3]*Advanced Photon Source, Argonne National Laboratory, Argonne, Illinois 60439*
[4]*Graduate School of Engineering Science, Osaka University, Toyonaka, Osaka 560-8531, Japan*
[5]*Japan Synchrotron Radiation Research Institute, Kouto 1-1-1, Mikazuki-cho, Sayo-gun, Hyogo 679-5198, Japan*
(Received 28 February 2002; published 26 April 2002)

Stroboscopic detection of nuclear forward-scattered synchrotron radiation is proposed and applied. Stroboscopic measurements provide energy-resolved spectra and relax the condition on the bunch mode. This concept is applied to study the magnetism in $CaFeO_3$ under high pressure.

DOI: 10.1103/PhysRevB.65.180404 PACS number(s): 76.80.+y, 41.60.Ap, 82.80.Ej

Nuclear resonant forward scattering of synchrotron radiation is a powerful technique to study hyperfine interactions.[1] It proved to be especially useful to study samples under extreme conditions, for example, in high-pressure experiments.[2] Contrary to a conventional radioactive source, synchrotron radiation has, even after monochromatization, a bandwidth that is of the order of 10^6 larger than the linewidth of most nuclear isomers. Consequently, synchrotron radiation is not energy selective for the different hyperfine levels, but excites all these levels coherently. Therefore, nuclear resonant scattering experiments are generally performed in a time-differential mode where the nuclear decay is investigated as a function of time after excitation by the synchrotron pulse. The quantum beats that are revealed in the forward-scattered radiation are the fingerprints of the hyperfine interactions.[3,4] In some cases, however, it may be difficult to record the nuclear scattering as a function of time, e.g., when the lifetime of the nuclear excited state is much longer than the synchrotron bunch interval. Alternative techniques have been proposed, such as the synchrotron Mössbauer source[5] for the study of ^{57}Fe samples, and, recently, the nuclear lighthouse effect[6] which can be applied to a wide range of isotopes. However, these techniques require that the sample is mounted on a Mössbauer drive or a rotor, respectively. In certain situations, this is technically difficult, e.g., when the sample is embedded in a high-pressure diamond anvil cell.

In this Communication, we introduce and demonstrate an alternative approach to record nuclear resonant scattered synchrotron radiation. The technique is based on the principles of stroboscopic acquisition and yields easily interpretable energy-resolved spectra. The new concept still takes advantage of the high brilliance, high degree of polarization, and strong intensity of the synchrotron radiation. It benefits from the time structure of the synchrotron radiation to suppress the detection of prompt nonresonantly scattered photons and to separate different stroboscopic resonances. The simplicity of the experimental setup (Fig. 1) allows us to investigate samples under extreme conditions, e.g., in a high-pressure diamond anvil cell. Similar to time-integrated synchrotron radiation spectroscopy,[7–9] there are two absorbers: the sample under investigation and an additional single-line absorber acting as a reference sample. This reference sample is mounted on a Mössbauer drive and scans the nuclear transition frequencies in the sample. In between the arrival of the prompt synchrotron pulses, delayed forward scattered radiation is recorded as a function of the velocity of the reference sample. In principle, any bunch mode is convenient, at the condition that the time resolution of the detector and the electronics is sufficient to isolate a time window with mainly delayed photons. Therefore, the technique is extremely favorable for the study of long-living Mössbauer isomers, e.g., ^{181}Ta. The key ingredients for stroboscopic detection of nuclear forward-scattered synchrotron radiation are appropriate tuning and periodicity of the time window.

Essential for stroboscopic measurements are a quantum beat with a variable frequency and a periodic time gating with a fixed frequency equal to the bunch frequency or a multiple of it. The quantum beat with variable frequency is provided by the interference between scattering in the sample under investigation and scattering in the reference sample. The tuning is established by changing the Doppler velocity of the reference sample. In the stroboscopic condition, the quantum beat frequency is equal to a multiple of the fixed time-window frequency. A well-chosen time window either selects the positive or the negative part of the quantum beat and a positive or negative resonance is created. If, on the other hand, the quantum beat is not in tune with the time window, positive and negative contributions will cancel each other. By recording the scattered intensity as a function of the Doppler velocity of the reference sample, an energy spectrum is obtained, similar to a Mössbauer spectrum. In the following, we will explain the stroboscopic idea in more detail and show experimental results on three different samples: $CaFeO_3$ in a high-pressure diamond anvil cell, stainless steel, and α-Fe.

The mathematical description of the stroboscopic resonances is based on the periodicity of the time-window func-

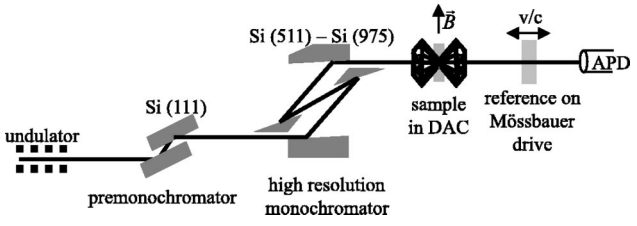

FIG. 1. Experimental setup.

tion $S(t)$. This function equals 1 or 0 if the data acquisition is on or off, respectively. Its period T corresponds to a frequency $\omega_T = 2\pi/T$. The periodicity of the function $S(t)$ allows an expansion in a Fourier series: $S(t) = \sum_{n=-\infty}^{+\infty} s_n \exp(in\omega_T t)$. Using this relation, the intensity as a function of the Doppler shift Δ, integrated over the allowed time window, can be calculated as

$$I_S(\Delta) = \sum_{n=-\infty}^{+\infty} \frac{s_n}{2\pi} \int_{-\infty}^{+\infty} d\omega \vec{A}(\omega,\Delta) \cdot \vec{A}(\omega + n\omega_T, \Delta). \quad (1)$$

$\vec{A}(\omega,\Delta)$ is the amplitude for a forward-scattered photon in frequency domain. In order to include the polarization dependence, $\vec{A}(\omega,\Delta)$ must be described by a two-component vector. The total scattering amplitude $\vec{A}(\omega,\Delta)$ contains three parts expressing nuclear resonant scattering in the sample under investigation ($f_s \vec{A}_{in}$), nuclear resonant scattering in the reference sample ($f_r \vec{A}_{in}$) and the radiative coupling ($f_s f_r \vec{A}_{in}$):[10]

$$\vec{A}(\omega,\Delta) = [f_s(\omega-\omega_i) + f_r(\omega-\omega_r-\Delta) + f_s(\omega-\omega_i) f_r(\omega-\omega_r-\Delta)]\vec{A}_{in}. \quad (2)$$

$\vec{A}_{in}$ is the amplitude of the incident broadband synchrotron photon, which can be considered as a constant. The resonance frequencies of the sample are given by ω_i, with $i = 1,N$ and N the number of allowed transitions. The reference frequency of the vibrating single-line sample is indicated by $\omega_r + \Delta$, with $\Delta = (v/c)\omega_r$ the variable Doppler shift. The nuclear resonant scattering factor f is in general polarization dependent and given by a 2 by 2 scattering matrix.[9] The scattering matrix f_s equals 0, except in the immediate vicinity of the resonance frequencies ω_i. If the intrinsic frequency of the time window, ω_T, is larger than the resonance frequency range, Eq. (1) can be simplified. Then, for each frequency ω, either the scattering matrix $f_s(\omega-\omega_i)$ or the shifted scattering matrix $f_s(\omega-\omega_i+n\omega_T)$ is 0 for $n \neq 0$. The same holds for the matrices $f_r(\omega-\omega_r-\Delta)$ and $f_r(\omega-\omega_r-\Delta+n\omega_T)$. Consequently, when substituting the amplitude of Eq. (2) in Eq. (1), for $n \neq 0$, all terms are canceled except for the pure interference terms [$I^n_{int}(\Delta)$ as defined below]. Using the relation $s_{-n} = s_n^*$, the intensity of Eq. (1) can now be written as

$$I_S(\Delta) = I^0(\Delta) + \sum_{n\neq 0} I^n_{int}(\Delta) \quad (3)$$

with

$$I^0(\Delta) = \frac{s_0}{2\pi} \int_{-\infty}^{+\infty} d\omega |\vec{A}(\omega,\Delta)|^2, \quad (4)$$

$$I^n_{int}(\Delta) = 2\Re\left(\frac{s_n}{2\pi} \int_{-\infty}^{+\infty} d\omega [f_s(\omega-\omega_i)\vec{A}_{in}] \cdot [f_r(\omega-\omega_r-\Delta+n\omega_T)\vec{A}_{in}] \right). \quad (5)$$

I^0/s_0 is the expression for the spectrum if no time gating were applied[7] and with the baseline due to the prompt photons subtracted. The remaining baseline is the velocity-independent intensity of the photons that are scattered either by the first or by the second absorber:

$$I^0_b = \frac{s_0}{2\pi} \int_{-\infty}^{+\infty} d\omega [|f_s(\omega-\omega_i)\vec{A}_{in}|^2 + |f_r(\omega-\omega_r)\vec{A}_{in}|^2]. \quad (6)$$

For $n=0$, the resonances consist of pure interference terms $I^0_{int}(\Delta)$, given by Eq. (5), and additional terms in which the radiative coupling of the amplitude [last term of Eq. (2)] is involved. The sign of these radiative coupling terms is opposite to the sign of the pure interference terms $I^0_{int}(\Delta)$,[10] and, therefore, the signal to baseline ratio will be reduced. $I^n_{int}(\Delta)$ for $n \neq 0$ describes the stroboscopic resonances of order n. These resonances are shifted by $v_n = n(\omega_T/\omega_r)c$ with respect to the central spectrum $I^0(\Delta)$. The larger the frequency ω_T or, equivalently, the smaller the period of the time window, the larger the shift of the different order spectra. As the terms $I^n_{int}(\Delta)$ contain no baseline or radiative coupling terms, they establish a pure interference spectrum, superposed on the baseline of the central spectrum. Consequently, the signal-to-baseline ratio in the stroboscopic resonances is of the order of $|s_n|/s_0$.

In order to give an explicit expression for $I_S(\Delta)$ we will consider the special case of thin single-line samples. If the effective thickness is much smaller than 1, the radiative coupling terms in $I^0(\Delta)$ can be neglected so that the spectrum is completely characterized by I^0_b and $I^n_{int}(\Delta)$. The scattering matrix f for a thin single-line sample can be replaced by a scalar scattering amplitude:

$$f_{s,r}(\omega-\omega_{1,r}) = iL_{s,r} \frac{\gamma/4}{(\omega-\omega_{1,r}-i\gamma/2)}.$$

.

Here, we introduced the effective thickness $L = \sigma_0 f_{LM} n d$ where σ_0 is the maximum resonance cross section, f_{LM} the Lamb-Mössbauer factor, n the density of resonant nuclei, and d the sample thickness. γ is the inverse of the Mössbauer lifetime. Using this expression for the scattering amplitude we obtain

$$I^0_b = s_0(L_s^2 + L_r^2)\frac{\gamma^2}{16}|\vec{A}_{in}|^2, \quad (7)$$

$$I^n_{int}(\Delta) = 2\Re\left(s_n \frac{\gamma + i(\Omega_n - \Delta)}{(\Omega_n-\Delta)^2+\gamma^2} \right) L_s L_r \frac{\gamma^2}{16}|\vec{A}_{in}|^2, \quad (8)$$

where $\Omega_n = \omega_1 - \omega_r + n\omega_T$.

Equation (8) shows that the shape of the stroboscopic resonances is a combination of Lorentzians and dispersions. However, if the time window is chosen symmetrically around $t_l = lT$, with $t=0$ being the arrival time of the prompt photons and l an integer, the coefficients s_n are real and the Lorentzian-like resonances are obtained. Depending on the sign of s_n, there is a reduction or an enhancement of the intensity. For thick absorbers, simulations have shown additional line broadening. Moreover, the radiative coupling terms can no longer be neglected so that the height of the central peak decreases. Therefore, for samples of arbitrary

thickness, it is more favorable to look for the stroboscopic resonances ($n \neq 0$) where the radiative coupling does not occur.

For nuclei with hyperfine split energy levels each resonance is replaced by a series of resonances according to the different frequencies ω_i. Note that, for a specific order, the relative position of these resonances is independent of the fundamental frequency ω_T of the time window and, hence, resembles a Mössbauer spectrum. Remark that, if the frequency ω_T of the time window is too small, different order spectra overlap. However, a proper analysis of the spectrum, which is based on Eq. (1), is still possible. Nevertheless, it is more convenient to increase the time-window frequency ω_T, resulting in a spectrum with a more straightforward interpretation.

We applied the stroboscopic concept at the nuclear resonant scattering beamline BL09XU in SPring-8, Japan.[11] The photons were detected by an avalanche photodiede detector with a time resolution of 0.3 ns and an efficiency of about 1%. The bunch interval was 23.6 ns. In the case of a resonance energy of 14.4 keV a time window with the same periodicity shifts the stroboscopic resonances by $v_n = n(\omega_T/\omega_r)c = n \times 3.65$ mm/s with respect to the central resonances. By selecting a time window with the double frequency, or equivalently, with a period of $T = 11.8$ ns, this shift is doubled to 7.3 mm/s. To obtain resonances with a Lorentzian shape, a symmetric time window around $t_l = l \times 11.8$ ns was selected. In a first approximation, the time window can be considered to be infinitely sharp so that the Fourier coefficients can be calculated analytically: $s_n = (-1)^n \sin(n\pi T_0/T)/n\pi$ with T_0 the duration of the time window. In order to suppress the second-order stroboscopic resonances, T_0 was fixed as $T_0 = T/2$ so that the Fourier coefficients are $s_0 = 0.5$, $s_1 = -0.318$, and $s_2 = 0$. This corresponds to a time window from 2.95 ns to 8.85 ns.

The technique will be demonstrated with an experiment on the perovskite iron oxide $CaFeO_3$ under high pressure. At ambient pressure, the high valent state of Fe^{4+} in $CaFeO_3$ shows a charge separation for temperatures below 290 K and an antiferromagnetic ordering for temperatures below 134 K. Under high pressure, the charge state of Fe is uniform and the magnetic ordering temperature rises above 300 K. Hence, at room temperature a sextet is found in the Mössbauer spectrum.[12] However, from an experiment without external magnetic field, it is impossible to distinguish between a ferromagnetic or an antiferromagnetic ordering. We will show that a small external field is able to align the Fe spins which proves the ferromagnetic ordering.

The $CaFeO_3$ was loaded in a diamond anvil cell (DAC) of the Basset type.[13] The pressure (42 GPa) was determined from the shift of the Ruby fluorescence lines.[14] An external magnetic field of 0.6 T was applied in the direction perpendicular to the polarization vector and to the propagation direction of the photon, as indicated in Fig. 1. For the reference sample we used enriched stainless steel (SS310) with an effective thickness $L_r = 15$. The count rate in the chosen time window was about 2.5 Hz. This low value can partly be attributed to the large absorption in the DAC and the low efficiency of the detector.

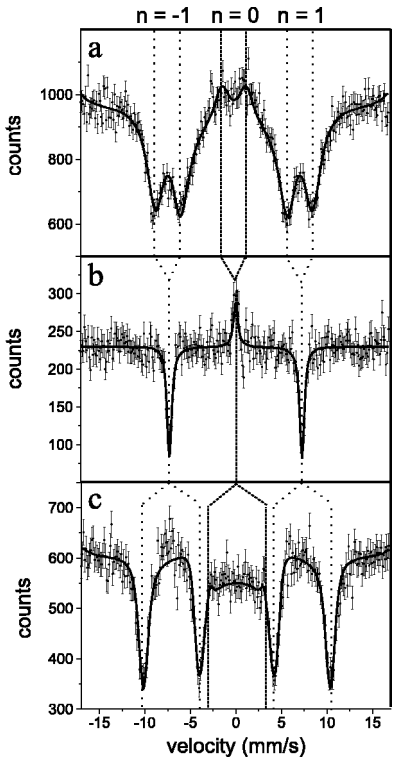

FIG. 2. Experimental results with a periodic time window (period $T = 11.8$ ns) from 2.95 ns to 8.85 ns. The solid line is a fit to the experimental data. The dotted lines indicate the different stroboscopic orders. (a) Enriched stainless steel (SS310) with effective thickness $L_r = 15$ and $CaFeO_3$ with effective thickness $L_s = 20$, under a pressure of 42 GPa with an external magnetic field of 0.6 T perpendicular to the polarization vector and to the propagation direction of the photon. (b) Two identical natural stainless steel (SS310) samples with effective thickness $L_s = L_r = 4.7$. (c) Enriched stainless steel (SS310) with effective thickness $L_r = 15$ and enriched α-Fe with effective thickness $L_s = 41$ in an external magnetic field of 0.25 T perpendicular to the polarization vector and to the propagation direction of the photon.

The spectrum obtained after 24 h of acquisition is shown in Fig. 2(a). In order to understand this spectrum, it is instructive to look at the result of similar measurements on two simpler and better known systems: stainless steel (SS310) and α-Fe under ambient conditions, the latter being subjected to an external magnetic field in the same direction as for the $CaFeO_3$. The results of these two measurements are shown in Figs. 2(b) and 2(c), respectively. In the case of SS310 [Fig. 2(b)] the spectrum nicely shows the stroboscopic resonances of zeroth and first order. Note that the signal-to-baseline ratio for the first-order resonances equals $|s_1|/s_0 = 0.63$. This is in agreement with Eqs. (5) and (6) using the identity $f_s = f_r$. This spectrum allows a calibration of the velocity scale. Since the resonance energies for both samples coincide, the zeroth-order resonance appears at $v = 0$ mm/s, while the first-order stroboscopic resonance should be at 7.3 mm/s. Using this calibration, the spectra of Figs. 2(a) and 2(c) were analyzed. Figure 2(c) shows the spectrum of α-Fe, obtained after an acquisition time of only 25 min. A comparison to the previous result reveals that each

resonance of Fig. 2(b) is now replaced by two resonances, indicating that there are two allowed transitions. This is in agreement with a hyperfine field perpendicular to the polarization vector and to the propagation direction of the photon so that only the two $\Delta m=0$ transitions are excited.[9,10] The separation of the resonances within each stroboscopic order is 6.0 mm/s that yields a total magnetic field value of 32.0(7) T. The isomer shift of α-Fe with respect to stainless steel was found to be 0.09(9) mm/s. Both values are in agreement with the values in the literature.[15] Note that the splitting is rather large so that the different order spectra are not completely separated using the present time gating. However, this did not affect the quality of the analysis. Note also that for the first-order resonances a signal-to-baseline ratio of about 0.4 is observed while the signal-to-baseline ratio of the central resonances is reduced due to the radiative coupling.

Returning to the $CaFeO_3$ measurement [Fig. 2(a)], we can now readily interpret the result. The spectrum shows two resonances in the first order (similar to the case of α-Fe) corresponding to the $\Delta m=0$ transitions. Hence, the small external magnetic field could align the spins and we conclude a ferromagnetic ordering of the Fe in $CaFeO_3$. A magnetic field value of 14.3(1.1) T and a shift of $-0.26(11)$ mm/s with respect to α-Fe was found. Both values are in agreement with earlier results.[12]

In conclusion, we developed and applied the concept of stroboscopic detection of nuclear forward-scattered synchrotron radiation. The technique can be applied to a wide range of isotopes and to various geometries and sample environments. The better the time resolution of the detector and the electronics the higher the time-window frequency and/or the bunch frequency can be. An optimal time window has a frequency that is larger than the resonance frequency range in the sample. A properly tuned symmetric time window gives rise to Lorentzian-like resonances, which makes the spectra readily interpretable. The interpretation of the stroboscopic resonances is very similar to the interpretation of a Mössbauer spectrum although their origin is quite different. Here, the resonances result from pure interference between two scattering paths that gives rise to a large signal-to-baseline ratio. The stroboscopic detection was applied for the first time to $CaFeO_3$ under high pressure. The experimental results showed that this new technique is very useful to extract reliable hyperfine interaction parameters.

R. Ca. and K. V. would like to thank the Belgian National Science Foundation (FWO-Vlaanderen) for financial support. This work was also supported by the IUAP program P4-07 financed by the Belgian Federal Office for Scientific, Technical and Cultural Affairs and a Grant-in-Aid for COE Research (10CE2004) from the Ministry of Education, Culture, Sports, Science and Technology of Japan. Work at Argonne was supported by U.S. Department of Energy, Office of Science, under Contract No. W-31-109-ENG-38. The experiments were performed at SPring-8 (experiment 2000B0045-NMD-np and 2000B0423-ND-np).

*Electronic address: riet.callens@fys.kuleuven.ac.be

[1] *Nuclear Resonant Scattering of Synchrotron Radiation (Part A)*, edited by E. Gerdau and H. de Waard [Hyperfine Interact. **123/124** (1999)], and references therein.

[2] R. Lübbers, G. Wortmann, and H.F. Grünsteudel, Hyperfine Interact. **123/124**, 529 (1999).

[3] G.T. Trammell and J.P. Hannon, Phys. Rev. B **18**, 165 (1978).

[4] E. Gerdau, R. Rüffer, R. Hollatz, and J.P. Hannon, Phys. Rev. Lett. **57**, 1141 (1986).

[5] G.V. Smirnov, U. van Bürck, A.I. Chumakov, A.Q.R. Baron, and R. Rüffer, Phys. Rev. B **55**, 5811 (1997).

[6] R. Röhlsberger, T.S. Toellner, W. Sturhahn, K.W. Quast, E.E. Alp, A. Bernhard, E. Burkel, O. Leupold, and E. Gerdau, Phys. Rev. Lett. **84**, 1007 (2000); R. Röhlsberger, K.W. Quast, T.S. Toellner, P.L. Lee, W. Sturhahn, E.E. Alp, and E. Burkel, *ibid.* **87**, 047601 (2001).

[7] R. Coussement, S. Cottenier, and C. L'abbé, Phys. Rev. B **54**, 16 003 (1996).

[8] C. L'abbé, R. Coussement, J. Odeurs, E.E. Alp, W. Sturhahn, T.S. Toellner, and C. Johnson, Phys. Rev. B **61**, 4181 (2000).

[9] R. Coussement, J. Odeurs, C. L'abbé, and G. Neyens, Hyperfine Interact. **125**, 113 (2000); C. L'abbé, R. Callens, and J. Odeurs, *ibid.* **135**, 275 (2001).

[10] G.V. Smirnov, Hyperfine Interact. **123-124**, 31 (1999).

[11] Y. Yoda, M. Yabashi, K. Izumi, X.W. Zhang, S. Kishimoto, S. Kitao, M. Seto, T. Mitsui, T. Harami, Y. Imai, and S. Kikuta, Nucl. Instrum. Methods Phys. Res. A **467**, 715 (2001).

[12] T. Kawakami, S. Nasu, T. Sasaki, S. Morimoto, S. Endo, S. Kawasaki, and M. Takano, J. Phys. Soc. Jpn. **70**, 1491 (2001).

[13] W.A. Basset, T. Takahashi, and P.W. Stook, Rev. Sci. Instrum. **38**, 37 (1967).

[14] H.K. Mao, P.M. Bell, J.W. Shaner, and D.J. Steinberg, J. Appl. Phys. **49**, 3276 (1978).

[15] N. Greenwood and T. Gibb, *Mössbauer Spectroscopy* (Chapman and Hall, London, 1971), p. 90.